CHAPTER 2

Gravity-Geologic Estimation of Bathymetry

Abstract

The gravity-geologic method for estimating bedrock elevation beneath unconsolidated materials was adapted for bathymetric determinations in the Barents Sea and the waters around Greenland. Control depths were used to determine regional gravity components that were removed from free-air gravity anomalies to estimate the gravity effects of the bathymetry. These gravity effects were converted to bathymetry by inversion, which in turn was compared to measured values to evaluate performance of the method. For the relatively shallow and high frequency bathymetry of the Barents Sea, the gravity-geologic predictions matched observed bathymetry with a ±26 meter RMS difference. Greater bathymetric variability was found in the deeper waters surrounding Greenland including the Greenland Sea, Labrador Sea, Davis Strait, and Baffin Bay. Predicted values here had a ±74 m RMS difference when compared at 257,941 known check points. These predictions represented a nearly 60% improvement over currently available bathymetry data sets, which includes JGP95E and EOTOPO5U digital elevation models. Additionally, these predictions were improved by nearly 40% when compared bathymetric predictions made by Smith and Sandwell

[1997]. Hence, bathymetric prediction by the gravity-geologic method can be effective for using gravity data to extend bathymetric coverage from limited shipborne soundings.

2.1 Introduction

The utility of the Gravity Geologic Method (GGM) was investigated in estimating improved bathymetry relative to seafloor elevations given by existing global EOTOPO5U and JGP95E models. By the GGM, the regional gravity field effect of the bathymetry is estimated from control station depths, such as provided by ship soundings, and removed from free-air gravity anomalies (FAGA). These anomalies may be estimated using satellite altimetry or directly measured by airborne and shipborne surveys.

For the Barents sea, bathymetric predictions were made using FAGA determined by Andersen and Knudsen [1998]. These data were derived from several satellite missions but were developed for the Barents Sea primarily from altimetry mapping of ERS-1 168-day mission. The track coverage from the ERS-1 mission was densest over the study area, thereby maximizing the resolution of FAGA and related bathymetric predictions.

The ERS-1 altimetry data were processed by Andersen and Knudsen [1998] so that most of the shorter wavelength components (< 40 km) were removed. Using procedures described in Appendix C, the short wavelength components were recovered and combined with the more regional gravity field of Andersen and Knudsen [1998]. Bathymetric determinations from the combined gravity data and the FAGA of Andersen and Knudsen [1998] were compared with bathymetric check values to

determine the magnitude of improvement that may be available from utilizing the enhanced gravity predictions. Comparison was also made with the EOTOPO5U and JGP95E global bathymetric models.

The flexibility of GGM to estimate bathymetry in regions of large depth variations was tested in the waters around Greenland. For the Greenland area, GGM predictions were derived only from the regional gravity field provided by Andersen and Knudsen [1998] and compared to the EOTOPO5U and JGP95E models. Additional comparisons were made with a bathymetry grid estimated only from the control depths and with the bathymetry of Smith and Sandwell [1997].

2.2 Review of the Gravity-Geologic Method (GGM)

As reviewed in Nagarajan [1994], the GGM was originally developed for predicting the depth to bedrock in regions overlain by lower density sediment and is outlined in Figure 2.1. The depth to the bedrock and the observed Bouguer gravity anomalies (BGA), known at control points (j), are used to produce a regional gravity field. The regional anomaly field is then subtracted from BGA at all other sites (i) to generate residuals that may be used to estimate the bedrock variations.

Variations in the local bedrock topography beneath a layer of unconsolidated sediment will generate a related high frequency gravity field (g_{BRT}), while all other more distant mass variations within the Earth will contribute to a regional gravity field (g_{REG}). These two components comprise the observed BGA (g_{OBS}) given by:

$$g_{OBS}(i) = g_{BRT}(i) + g_{REG}(i) \tag{2.1}$$

The bedrock gravity effect is estimated using the following Bouguer slab formula:

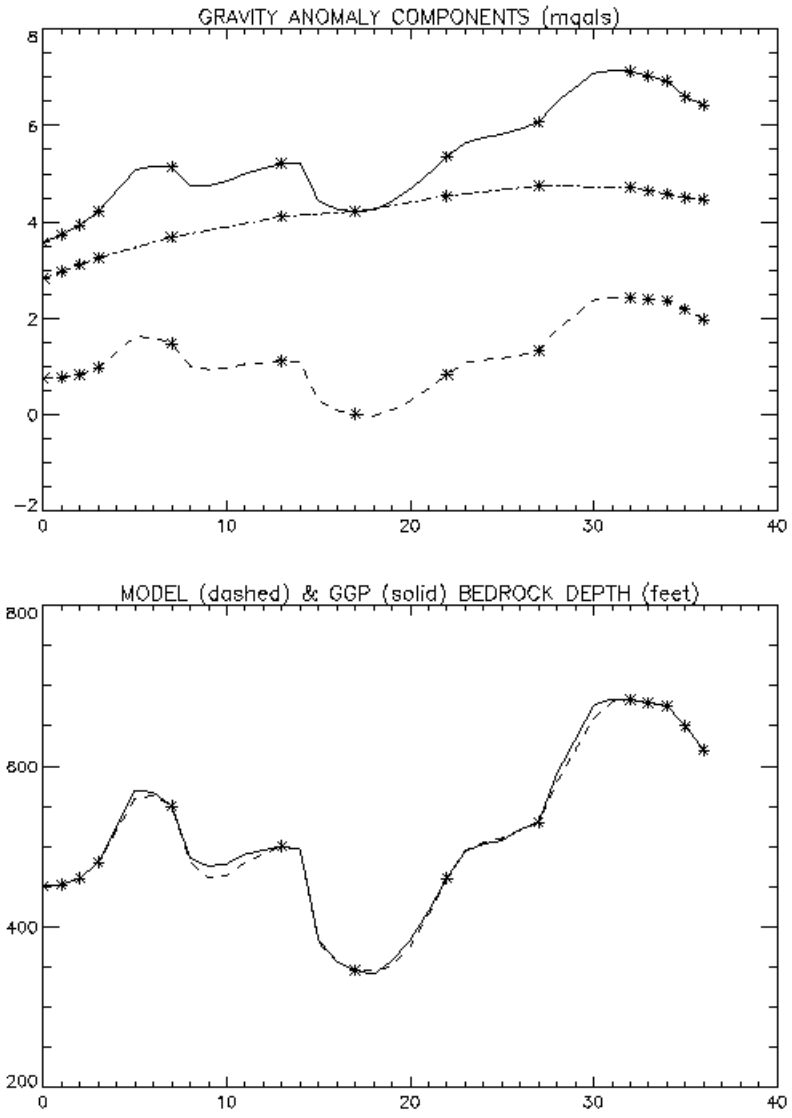

Figure 2.1: The Gravity-Geologic-Method (adapted from Figure 3 of Nagarajan [1994]). The top panel shows the gravity field components: observed anomalies (solid= $g_{OBS}(i)$), regional anomalies (dash-dot= $g_{REG}(i)$), and bedrock-topography anomalies (dashed= $g_{BRT}(i)$). The bottom panel shows the original model (dashed) and that predicted by GGM (solid). Asterisks (*) mark the 14 control measurement locations used in making predictions at all 37 points. A density contrast of 0.56 gm/cm^3 was assumed between the rock and sediment layer.

$$g_{BRT}(j) = 2\pi G\Delta\rho\,(E(j) - D) \tag{2.2}$$

where: G= $6.672 \cdot 10^{-8} \frac{cm^3}{gm \cdot s^2}$;
$\Delta\rho$ = density contrast = 0.56 g/cm^3);
$E(j)$ = bedrock elevation (m) at jth control point; and
D = reference datum elevation (m)

The bedrock elevations are determined by borehole measurements through the overlying unconsolidated sediment. The deepest measurement is commonly used as the reference datum (D). The gravity effect of the bedrock surface at the borehole locations is estimated by Equation 2.2 and removed from the original BGA values to yield the following regional gravity effects:

$$g_{REG}(j) = g_{OBS}(j) - g_{BRT}(j) \tag{2.3}$$

The regional estimates determined at the sample sites (boreholes) are interpolated or gridded to generate a regional anomaly map and removed from the original BGA to generate bedrock anomalies over the original grid:

$$g_{BRT}(i) = g_{OBS}(i) - g_{REG}(i) \tag{2.4}$$

By rearranging the terms in Equation 2.2, these bedrock anomalies may be used to estimate the bedrock surface variations according to:

$$E(i) = \frac{g_{BRT}(i)}{2\pi G\Delta\rho + D} \tag{2.5}$$

Errors in this inversion are controlled by the accuracies to which $g_{OBS}(j)$, $g_{BRT}(j)$, and $g_{REG}(j)$ are determined. Survey positioning and data reduction accuracies propagate into errors in g_{OBS}, while the distribution of g_{OBS} must also be adequate to resolve topographic details effectively. Errors in g_{BRT} depend on errors in the control elevations and related Bouguer slab modeling. The effectiveness of g_{REG} is facilitated

by a regional gravity anomaly which is sufficiently simple that the control points yield accurate estimates at the observation points. Errors in density estimates propagate through the Bouguer slab approximations (e.g., Equations 2.2 and 2.5). In general, the accuracy of GGM estimates of bedrock topography are primarily influenced by the number and distribution of elevation control points and the density contrasts between bedrock and the overlying sediments [Nagarajan, 1994]. However, as described by Nagarajan [1994], methods may be readily devised to test these parameters in any application by studying their effects on a subset of the control points.

Error assessment of this method may be made by retaining a portion of the control points back as check values. Values determined by the GGM may be compared to actual depth values for a known depth.

An attractive application for this method is predicting the ocean bottom beneath a layer of sea water. In the marine application, bathymetry predictions are made instead of depths to bedrock and FAGA are used instead of BGA, but the process otherwise remains the same. Over ocean areas, FAGA replace BGA because the FAGA are located approximately at the geoid and, hence, do not need to be corrected for free-air and Bouguer mass effects. Also, the assumption of homogeneity in the density contrast across the bedrock interface is more valid in marine rather than terrestrial applications. In terrestrial applications, GGM predictions may be seriously distorted because density variations within the overlying unconsolidated materials and bedrock may be the same order of magnitude or greater than the density contrast at the bedrock interface [Ibrahim and Hinze, 1972; Adams and Hinze, 1995; Anderson, 1991; Nagarajan, 1994]. Relative to marine applications, the density contrast between seawater and bathymetry is much more dominant and homogeneous.

The utility of the GGM for predicting bathymetry is evaluated in the following sections. It is adapted from Nagarajan [1994] and modified for marine application

in both the shallow environment of the Barents Sea and the deep sea environment around Greenland.

2.3 Application of the GGM in the Barents Sea

To test the GGM in a shallow sea environment, the area 74.000 - 76.116°N and 43.000 - 51.466°E in the Barents Sea was selected, because it is well covered by satellite altimetry and bathymetric data from ship soundings (Figure 2.4). The ERS-1 168 day mission altimetry coverage was used to enhance the higher frequency components of the FAGA anomalies from Andersen and Knudsen [1998] that are shown in Figure 2.2. As described in Appendix C, the ERS-1 track spacing of about 2 to 3 km between tracks for this region yielded enhanced FAGA estimates at an optimal 5 km spatial resolution as shown in Figure 2.3.

Additionally, bathymetric measurements digitized by the Naval Research Laboratory from USSR charts and Norwegian Polar Institute charts were obtained (Robin Warnken, pers. comm., 1997). These data provide both the control necessary to generate the bathymetric estimates along with test values to check the validity of the estimates. Of the 327 bathymetric measurements for this region, two thirds of these points (218) were used as control depths, as shown in Figure 2.4, with the remaining values (109) retained as check points. These data were collected along profiles where every third point was used as a check point to ensure fairly even distribution of check points across the study area.

As mentioned in the previous section, density is involved in the denominator of Equation 2.5, so that small errors in the density contrast assumptions can substantially amplify errors in the residual gravity anomalies and, hence, in the bathymetric predictions. However, Nagarajan [1994] found that the check points can be used to

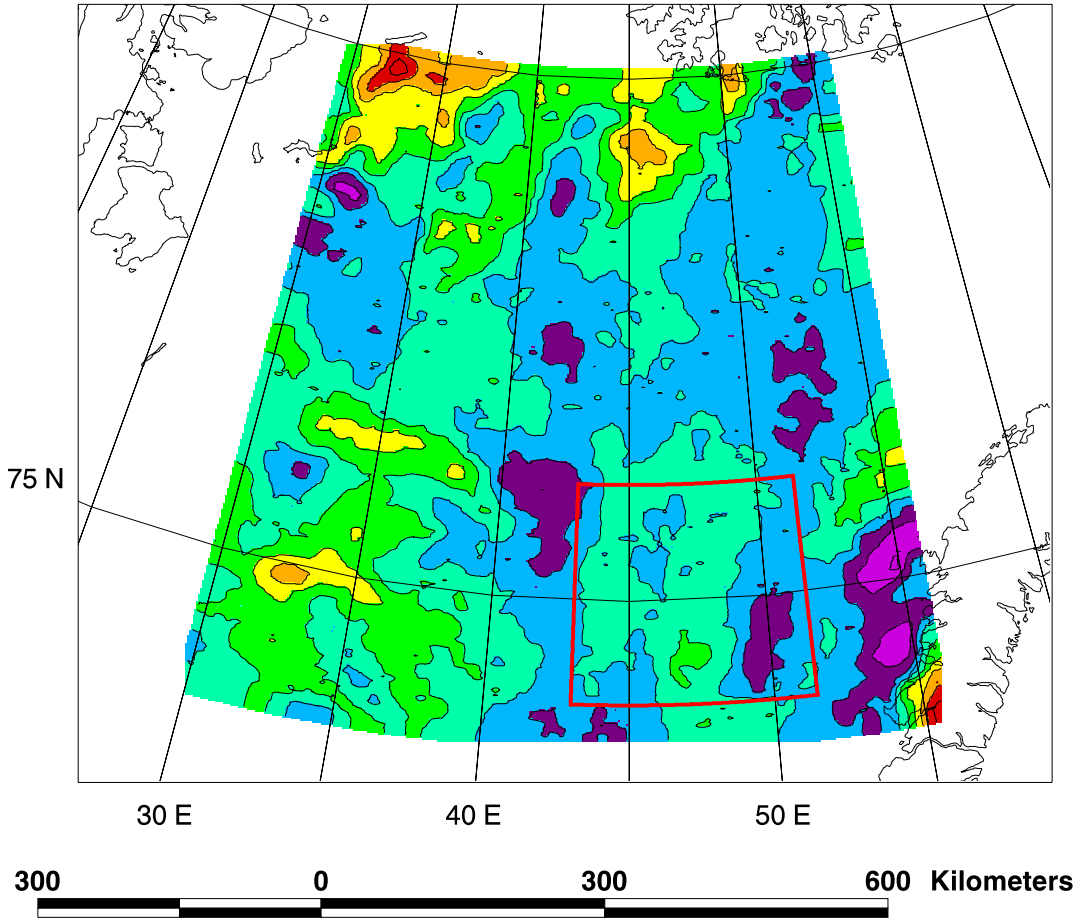

Figure 2.2: Standard FAGA from Andersen and Knudsen [1998] (g_{OBS}) for the Barents Sea in a Lambert Equal-Area Azimuthal Projection centered on 45 E at sea level. The test area is delineated by the red box.

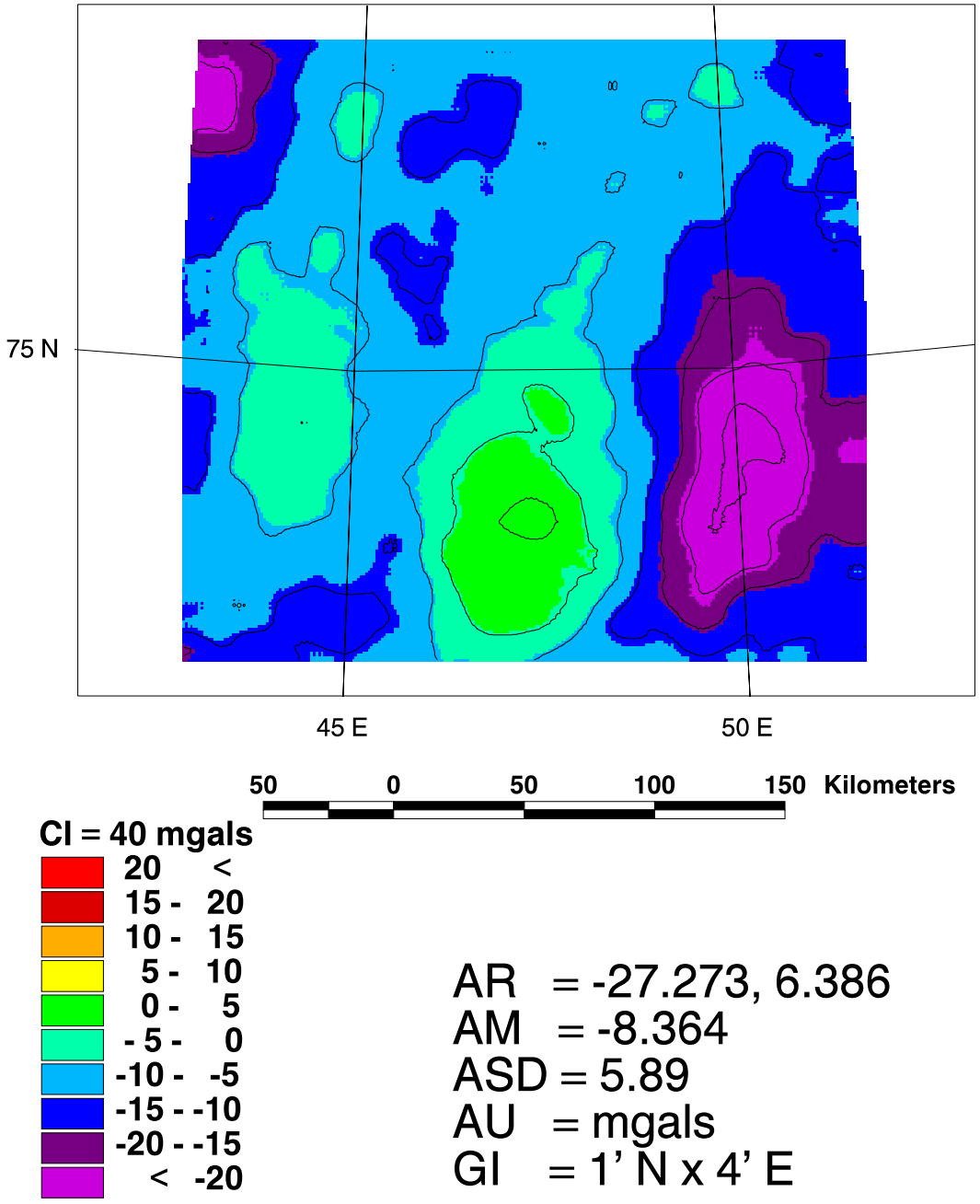

Figure 2.3: FAGA from Andersen and Knudsen [1998] with enhanced high frequency components for the study area (g_{OBS}) outlined in Figure 2.2. These data for the Barents Sea are shown in a Lambert Equal-Area Azimuthal Projection centered on 47°E at sea level.

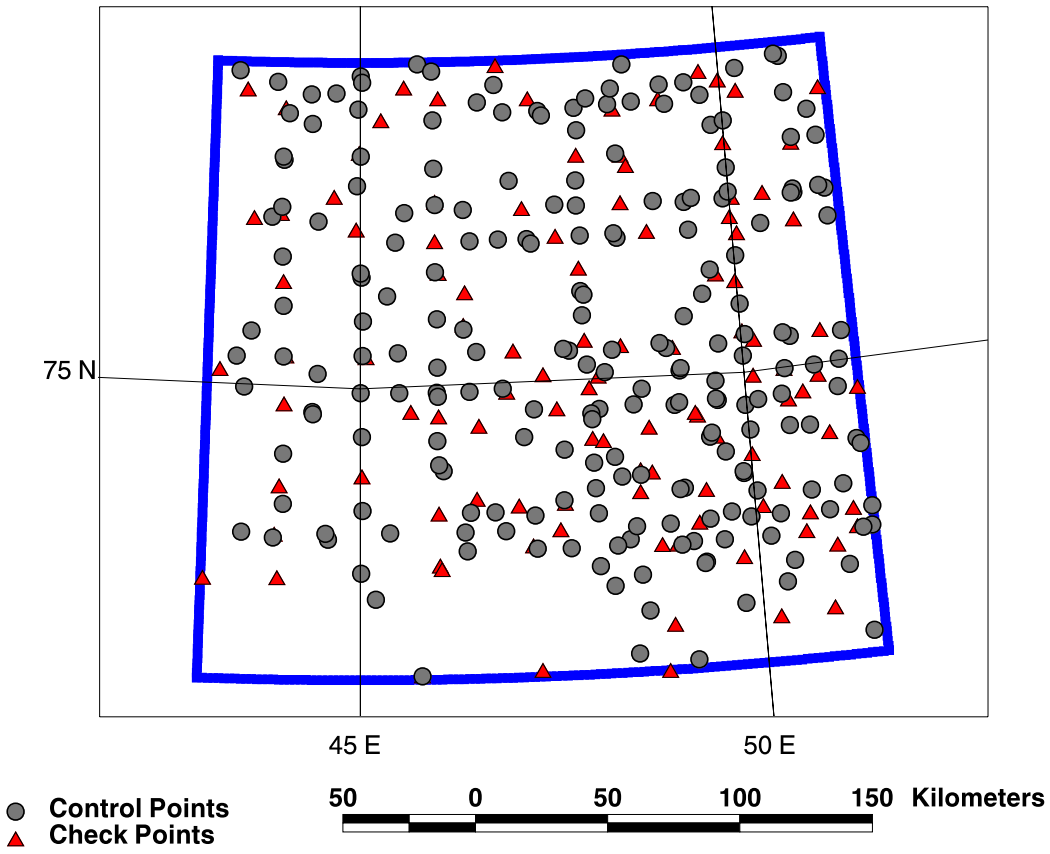

Figure 2.4: Barents Sea bathymetric control and check points within the study area outlined in Figure 2.2. Data were digitized by NRL from USSR charts and Norwegian Polar Institute charts. The blue outline box delineates the field area, grey circles denote control bathymetry, and red triangles denote check points.

choose an optimum (although not geologically realistic) value for $\Delta\rho$ in any application.

The implementation of this procedure for the study region is given by the trade-off diagram in Figure 2.5. The curves give variations in the agreement (correlation coefficient) and disagreement (RMS difference) between the predictions and the check points with changes in the density contrast assumed between seawater and bathymetry. At the geologically reasonable value of 1.7 gm/cm^3, the curves indicate that the predictions match only about 23% of the check points and have an RMS difference of about 144 m with all check points. However, the match significantly improved as the density contrast is increased, so that at 20.0 gm/cm^3 the predictions match nearly 79% of the check points with an RMS difference of about 26 m. Although not a geologically reasonable value, assuming a density of 20.0 gm/cm^3 does sharpen the contrast between the sediment and bedrock and permit a higher resolution for determining varying bathymetry over a relatively narrow range of values (a few 100's m). Therefore, this value was implemented for the density contrast used to make the bathymetric predictions in the study area.

Using 20.0 gm/cm^3, the regional grid was determined from the control data as shown in Figure 2.6. The regional anomaly field was removed from the enhanced FAGA grid to generate a residual FAGA grid given in Figure 2.7. These residual anomalies were directly interpreted for the bathymetry that is given in Figure 2.8.

To study the utility in using the FAGA where the high frequency components have been enhanced to obtain improved bathymetric estimates, GGM predictions were developed using only the FAGA from Andersen and Knudsen [1998]. The resultant bathymetric predictions are given in Figure 2.9. Also for comparison, the 218 control points were gridded into a bathymetric map as shown in Figure 2.10 using

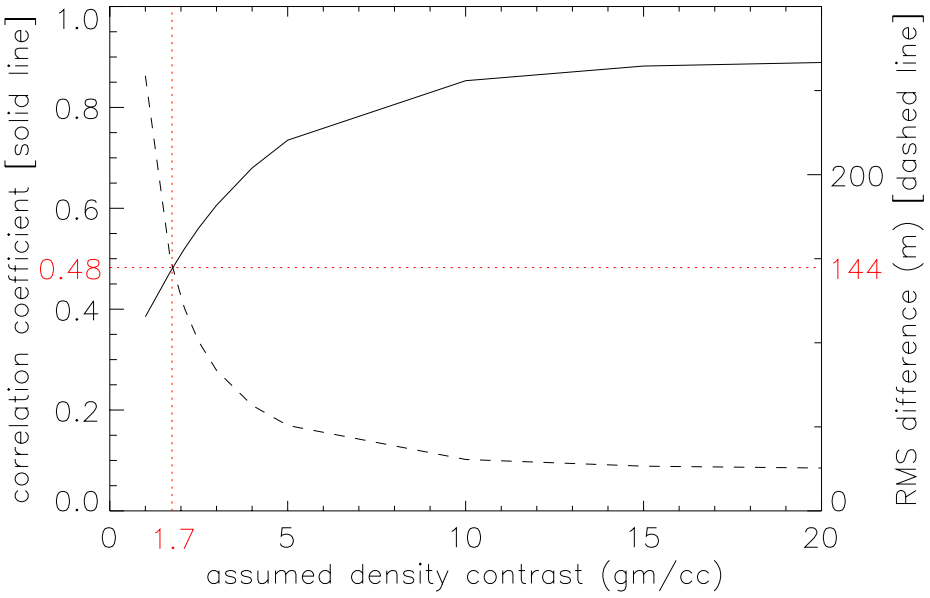

Figure 2.5: Trade-off diagram for choosing an effective density contrast in GGM predictions of bathymetry for the Barents Sea study area. Solid and dashed curves give the correlation coefficient and RMS difference, respectively, between the predictions and the check points as a function of varying density contrasts. The trade-off diagram indicates that little improvement may be expected from predictions based on density contrasts greater than 20.0 gm/cm^3. Lower values up to about 10.0 gm/cm^3 may provide higher resolution predictions with marginal decrease in statistical performance. A geologically more reasonable density contrast of 1.7 gm/cm^3 (intersection of the red dotted lines) does not perform well, matching only 23% of the check points and having an RMS difference of 144 m.

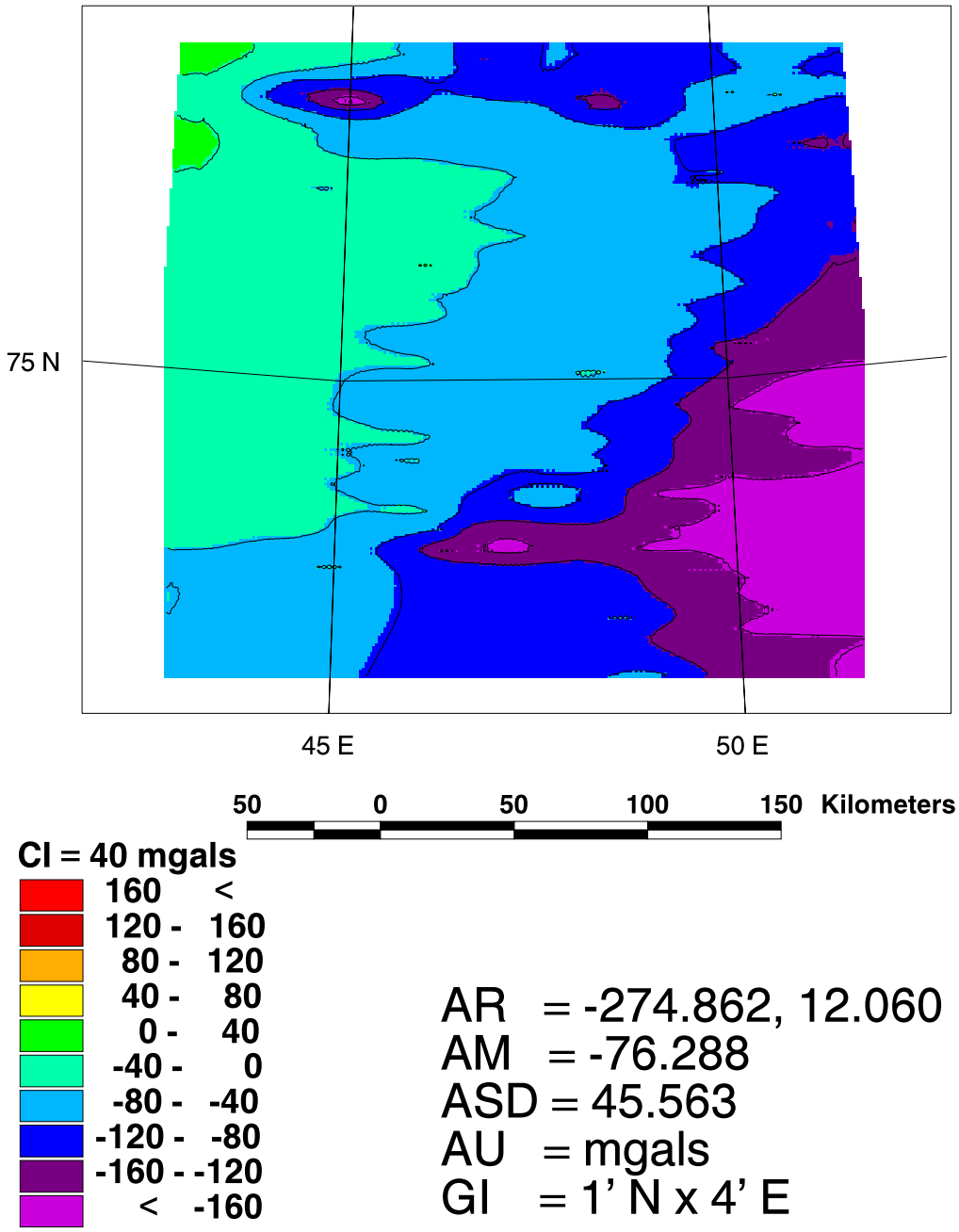

Figure 2.6: Regional gravity anomalies (g_{REG}) determined from control points in the bathymetry for the Barents Sea study area. The data are shown in a Lambert Equal-Area Azimuthal Projection centered on 47°E at sea level.

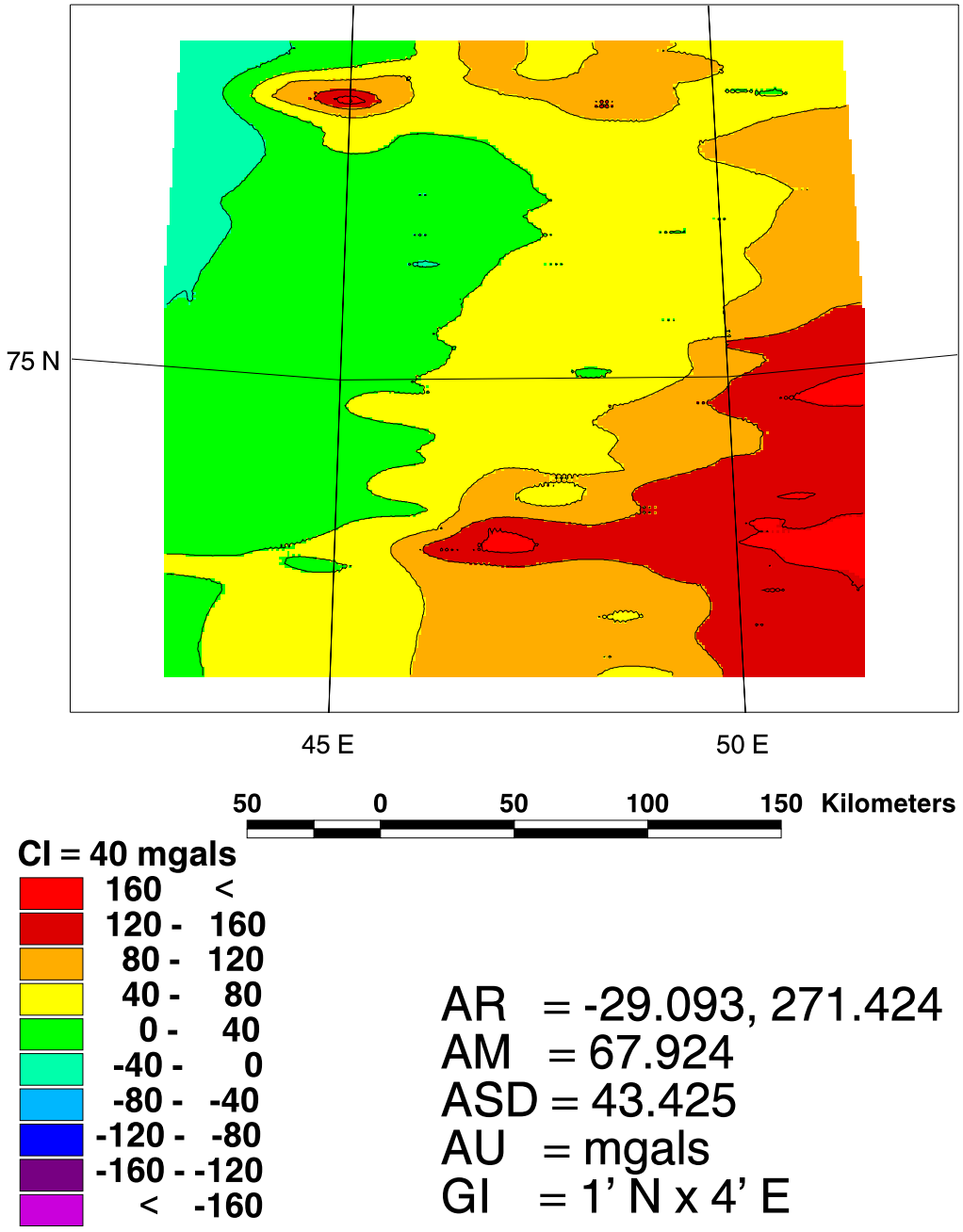

Figure 2.7: Residual gravity anomalies (g_{BRT}) for the Barents Sea study area shown in a Lambert Equal-Area Azimuthal Projection centered on 47°E at sea level. These anomalies were the result of removing the regional gravity effects (g_{REG}) shown in Figure 2.6 from the enhanced FAGA (g_{OBS}) shown in Figure 2.3.

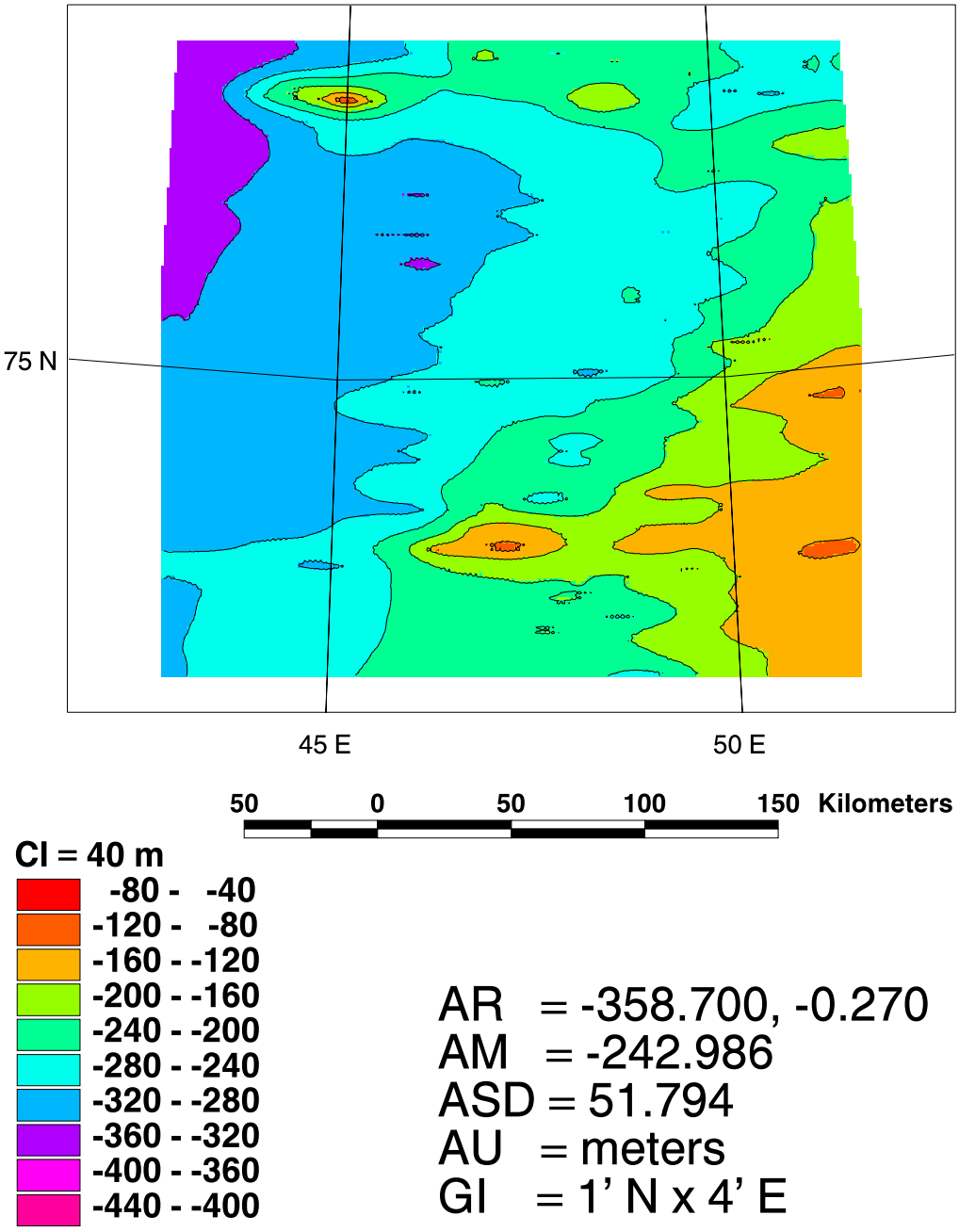

Figure 2.8: GGM bathymetric predictions from enhanced FAGA for the Barents Sea. The data are shown in a Lambert Equal-Area Azimuthal Projection centered on 47°E at sea level.

a standard minimum curvature algorithm [Smith and Wessel, 1990]. Finally, bathymetric estimates determined from the EOTOPO5U and JGP95E data sets are shown in Figures 2.11 and 2.12, respectively.

These five sets of bathymetric predictions were next correlated with the 109 check points to quantify the phase and magnitude of mismatch in terms of the correlation coefficient and RMS difference, respectively. The results of this comparison are given in Table 2.1. The bathymetry determined from simply gridding the control points correlated with the check points at 0.83 and had an RMS difference of 31 m. GGM-derived bathymetry using the standard FAGA from Andersen and Knudsen [1998] correlated at 0.89 and had an RMS difference of 26 m. Likewise, the GGM-derived bathymetry using the enhanced FAGA had nearly identical results.

The bathymetric predictions determined using either standard FAGA or enhanced FAGA appear to be identical (CC=1.00), but the use of the enhanced FAGA improved the correlation coefficient minutely. The enhancement of the FAGA was performed using ERS-1 altimetry (see Appendix C), which has been noted in Yale et al. [1995] as having a lower signal resolution than GEOSAT altimetry. This variability is such that 20 km is the effective wavelength resolution employed by Sandwell and Smith [1997] in determining their FAGA from ERS-1 and GEOSAT altimetry. As GEOSAT altimetry is not available above 72°N, ERS-1 altimetry was used and low pass filtered at a 16 km wavelength to determine the most optimal signal. This optimization was determined based upon the comparison of the GGM-derived bathymetry from the enhanced FAGA with the check points. The 16 km filter most probably removed signal as well as noise and reduced the effectiveness of the enhancement techniques. When GEOSAT altimetry was tested in another area further south, the optimal filtering level was determined to be about 12 km, and significant small scale features were determined at this resolution [Roman, 1996; Roman and von Frese, 1998a].

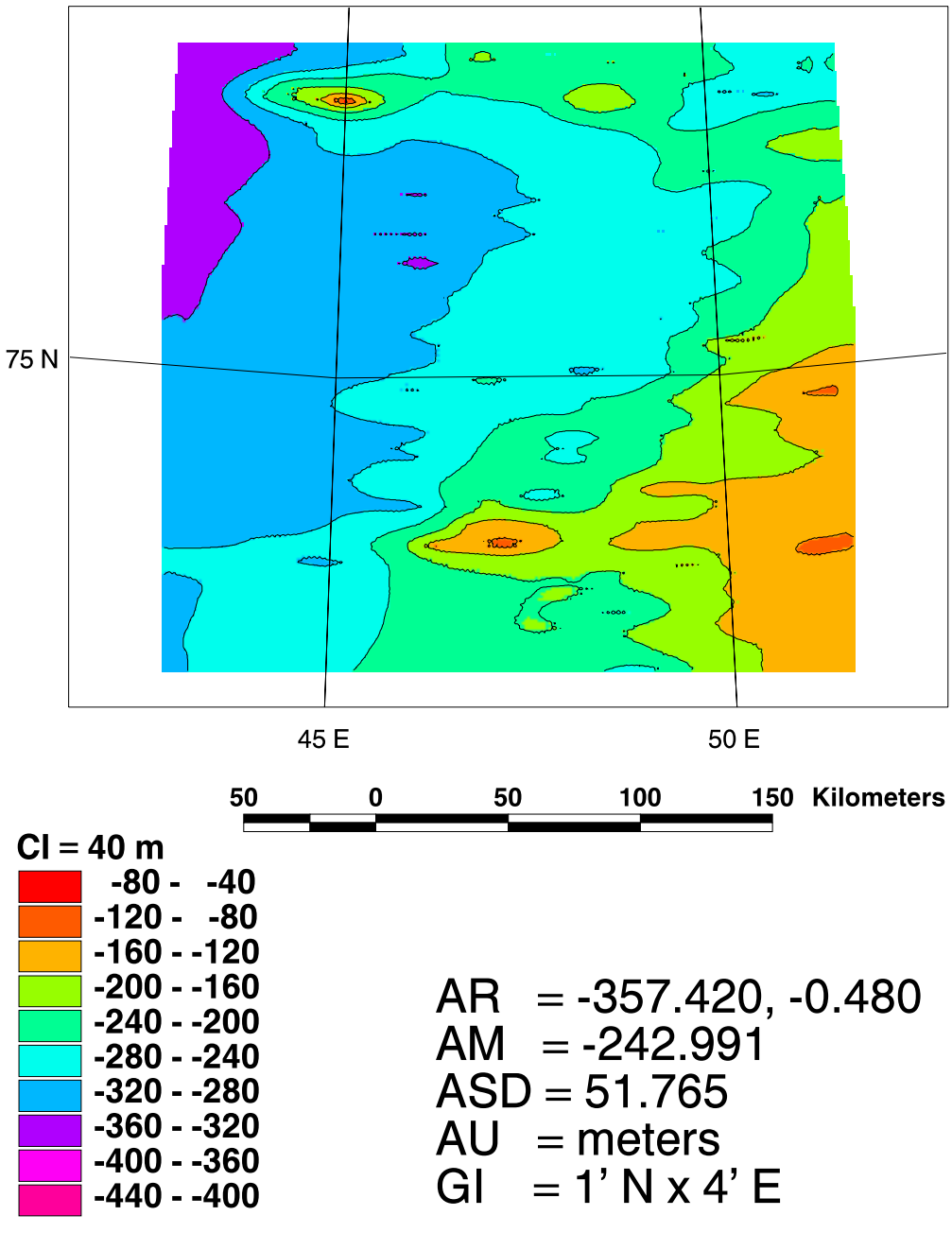

Figure 2.9: GGM bathymetric predictions from standard FAGA of Andersen and Knudsen [1998] for the Barents Sea study area. The data are shown in a Lambert Equal-Area Azimuthal Projection centered on 47°E at sea level.

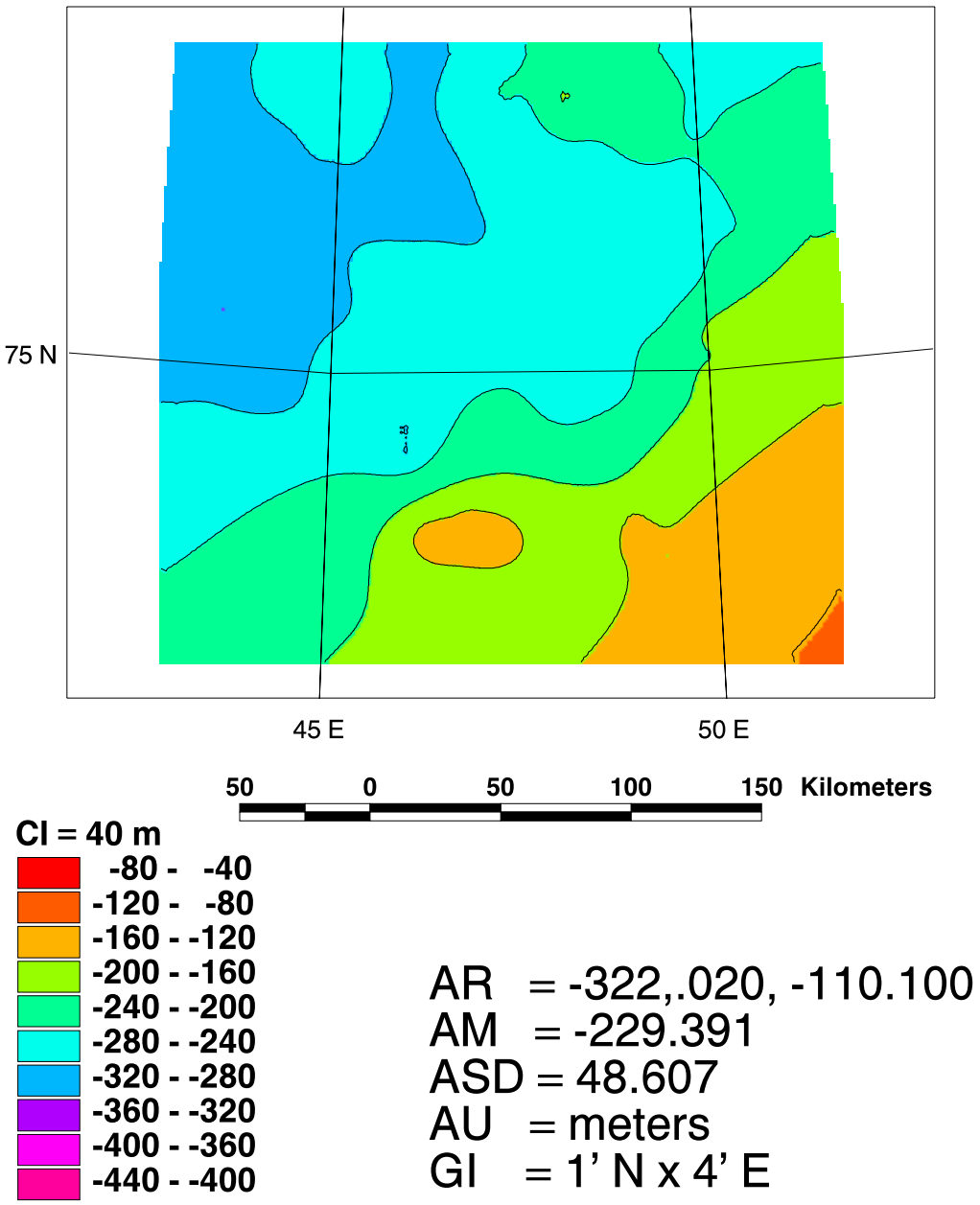

Figure 2.10: Bathymetry estimated from gridding the 218 control points for the Barents Sea study area. These data are shown in a Lambert Equal-Area Azimuthal Projection centered on 47°E at sea level.

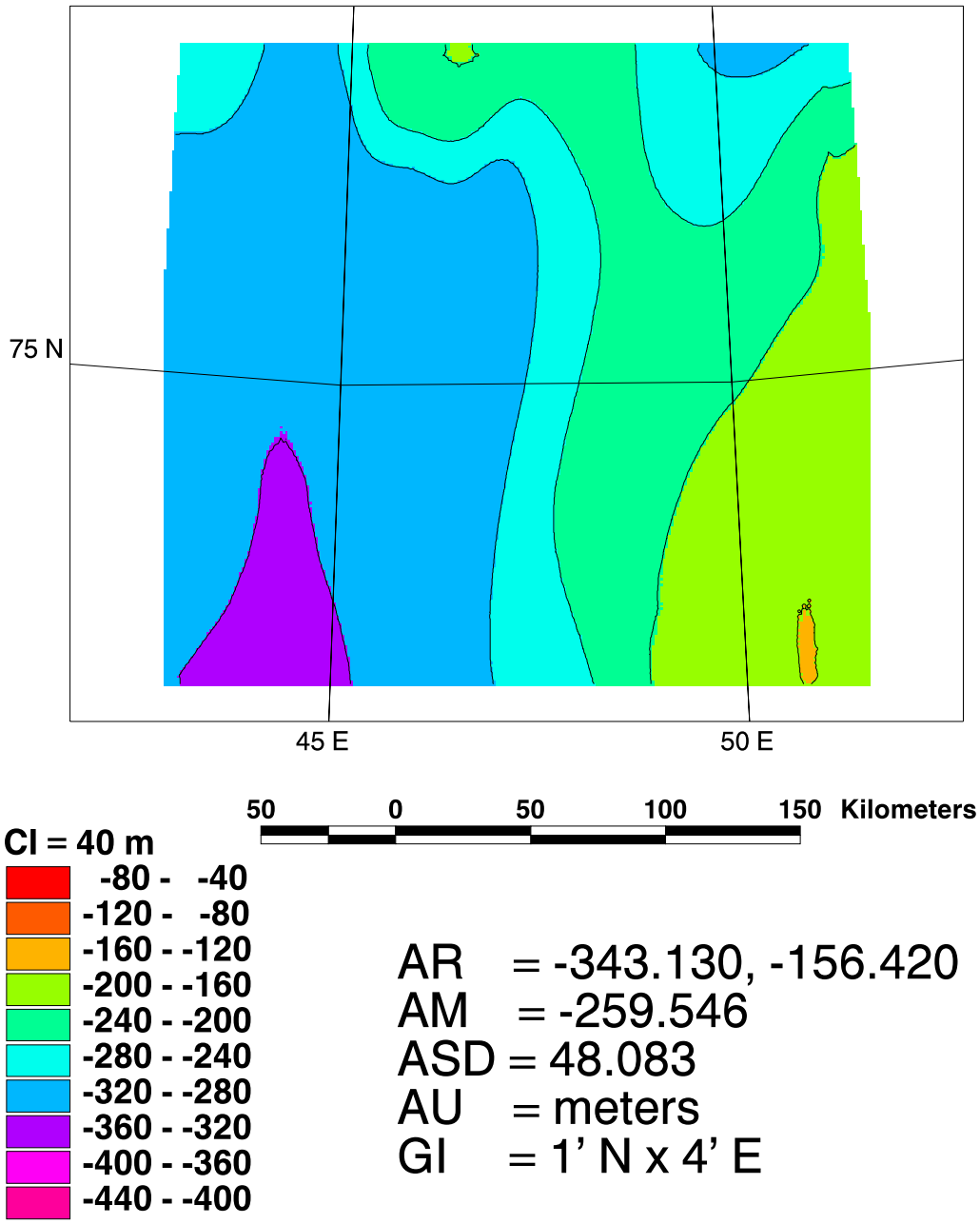

Figure 2.11: EOTOPO5U bathymetry for the Barents Sea in a Lambert Equal-Area Azimuthal Projection centered on 47°E at sea level.

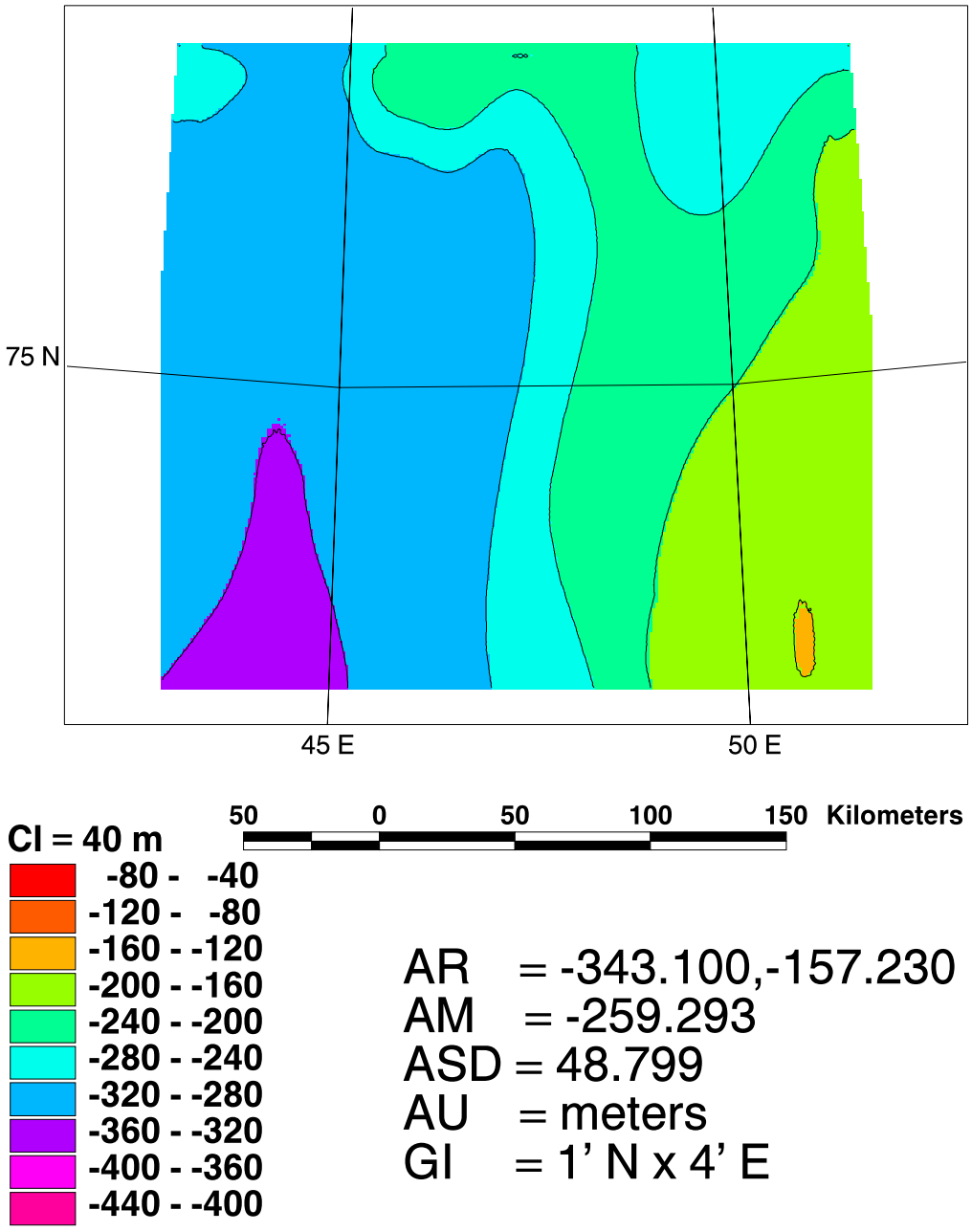

Figure 2.12: JGP95E bathymetry for the Barents Sea in a Lambert Equal-Area Azimuthal Projection centered on 47°E at sea level.

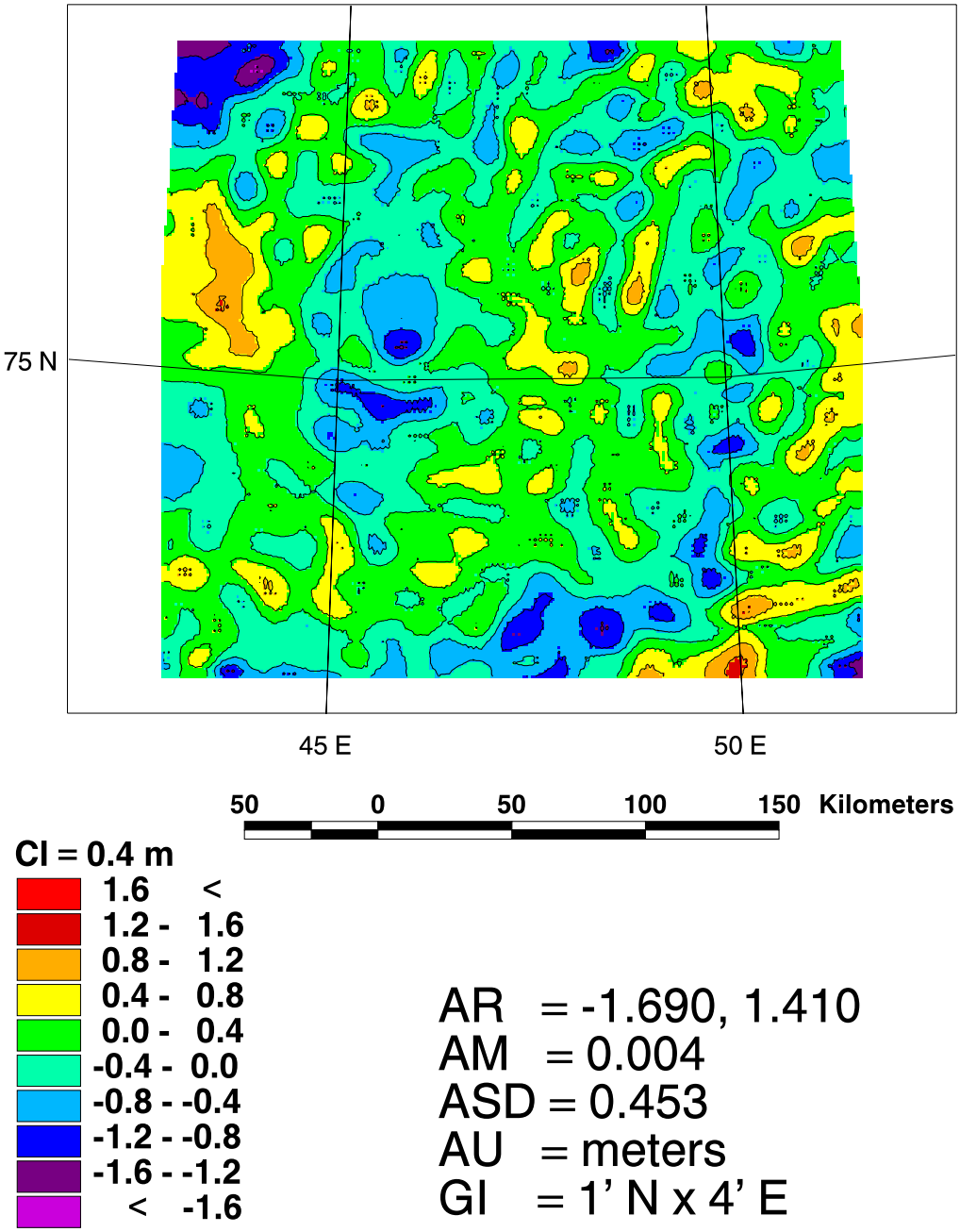

Figure 2.13: Bathymetric differences obtained by subtracting the standard FAGA predictions (Figure 2.9) from the enhanced FAGA (Figure 2.8) for the Barents Sea study area. Data are shown in a Lambert Equal-Area Azimuthal Projection centered on 47°E at sea level.

The difference between the GGM-predictions determined from standard and enhanced FAGA is given in Figure 2.13 and shows fairly insignificant features of less than 2 meters magnitude. Given the 26 meter RMS difference when compared to the check points, the enhanced FAGA do not add a significant component to the bathymetric predictions.

The JGP95E and EOTOPO5U bathymetry compared less favorably than the GGM-predicted bathymetry from either standard or enhanced FAGA. Also, the results for the GGM-bathymetry were more favorable than that for the gridded control data (CC = 0.83) possibly due to the sparsity of the control data. However, Both GGM-predictions generated a significant shallow feature in the northwest region not observed in the control data or check points. This shallow feature occurs near the edge and represents the highest bathymetric prediction for either the enhanced or standard FAGA derived GGM-predictions. For both GGM-predictions, this feature may possibly represent an edge effect created during the generation of the regional gravity field which then propagated into the bathymetric predictions.

All predictions show the same general long wavelength trend in the bathymetry (all CC's are greater than 0.77), but the GGM-predictions and the gridded control data show more detail and better predict the bathymetry based upon the comparison with the check points. Because there was little improvement using the enhanced FAGA over the standard FAGA, the use of only standard FAGA models seem to be sufficient and effective for estimating shallow water bathymetry.

The next section investigates the use of standard FAGA for making GGM-predictions of bathymetry in the deeper marine environment of Greenland. Global bathymetric models also provide estimates for these waters that will be compared.

bathymetric data set	CC	RMS diff. (meters)	mean diff. (meters)	improvement. factor
enhanced FAGA GGM-derived	0.890	25.5	-1.7	-
standard FAGA GGM-derived	0.889	25.5	-1.8	-
EOTOPO5U	0.774	35.3	17.6	28%
JGP95E	0.781	34.9	16.2	27%
gridded control data	0.834	30.8	-4.5	17%

Table 2.1: Comparison of bathymetric models for the Barents Sea using enhanced gravity GGM-derived, standard gravity GGM-derived [Andersen and Knudsen, 1998], EOTOPO5U DEM, JGP95E DEM, and gridded control data. The control data consist of 218 points, while all models are statistically compared to 109 check points. The field area ranges from 43.000 to 51.467°N and 74.000 to 76.116°E. Statistics of the comparison include overall correlation (CC), the RMS of the differences, and the mean difference. Lastly, an improvement factor with respect to the GGM-derived bathymetry is given to demonstrate the magnitude of the improvement $= \frac{RMS_i - RMS_{GGM}}{RMS_i}$.

2.4 Application of the GGM in the Greenland Area

The increased anomaly resolution that is reflected by the enhanced FAGA had little impact upon the estimation of bathymetry in shallow waters. For deep water regions, use of enhanced FAGA are likely to have even less impact due to attenuation of the gravity effects of the bathymetry. For example, water depths on the abyssal plains can reach 4 to 5 km, so that the gravity effects by the bathymetry will be of the order of 8 to 10 km and larger. Because significant portions of the oceans are deeper than 1 km, the enhanced FAGA are not likely to yield greatly improved bathymetric predictions over those from the standard FAGA provided by Andersen and Knudsen [1998].

For the marine areas of Greenland, 224,493 bathymetry points were obtained from the Geological Survey of Canada (GSC). As shown in Figure 2.14, these data cover the Arctic Sea, Nares Strait, Baffin Bay, and the Davis and Labrador Straits. Also

shown in Figure 2.14 are an additional 291,387 bathymetry points covering the East Greenland Sea and Fram Strait that were obtained from the TRKDAS data set of the National Geophysical Data Center's (NGDC). The two data sets overlap by about 300 km off of southern Greenland. These combined data sets represent 515,880 points that were split into a group of 257,939 control points for the determination of the regional FAGA field (g_{REG}) and a group of 257,941 check points for testing the accuracy of the resulting bathymetry.

Roughly 73% of the GSC data had observation error information, for which the mean RMS error was about 35 meters. Error estimates for the bathymetry were not explicitly given for the TRKDAS data but were assumed to be of the same quality as the GSC data.

An effective density contrast was determined by an analysis similar to the one performed for the Barents Sea predictions in Figure 2.5. The results for the deep water application suggested that a value of 2.06 gm/cm^3 (= 3.1 (oceanic bedrock) - 1.04 (sea water)) was adequate.

The regional gravity field (g_{REG}) generated from the control data are given in Figure 2.15. These regional effects were removed from the standard FAGA for this region given in Figure 2.16. The FAGA from Andersen and Knudsen [1998] were utilized because these predictions extend to 80°N, in contrast to the FAGA from Sandwell and Smith [1997] that only extend to 72°N. The residual FAGA are shown in Figure 2.17, and the bathymetry predictions determined from these residual FAGA are given in Figure 2.18.

For comparison, predictions from the EOTOPO5U and JGP95E models are given in Figures 2.19 and 2.20, respectively. All control points were also gridded using minimum curvature to generate the bathymetric predictions given in Figure 2.21.

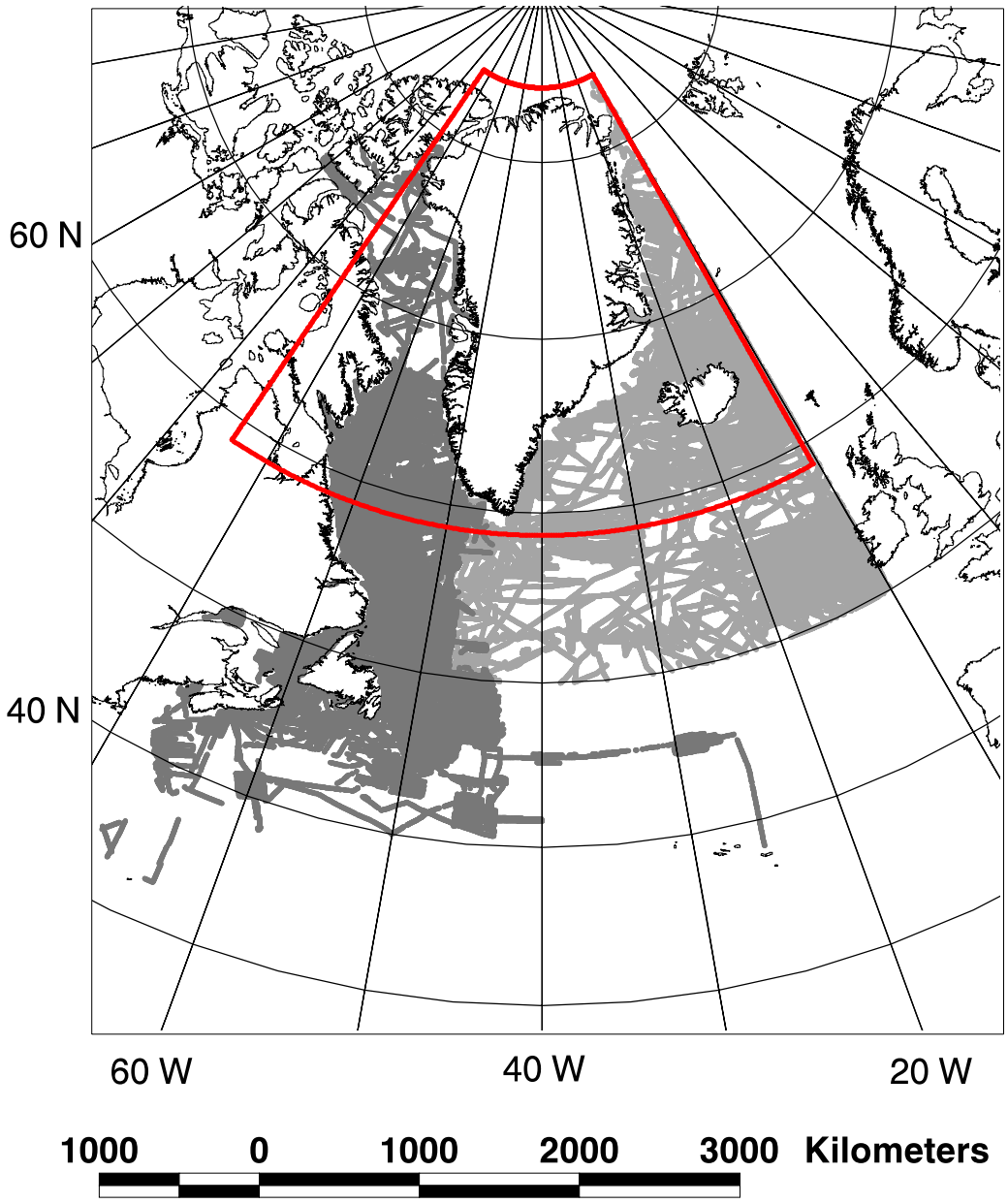

Figure 2.14: Greenland bathymetric control and check values shown in a Lambert Equal-Area Azimuthal Projection centered on 40°W. Data coverage includes 291,387 points mainly in the eastern areas from the NGDC and 224,493 points mainly in the western areas from GSC (darker grey). The study area around Greenland is also delineated.

bathymetric data set	coverage (degrees)	CC	RMS diff. (meters)	mean diff. (meters)	percent (%) improvement
GGM	90-0 W 40-80 N	0.998	73.7	-2.3	-
EOTOPO5U	90-0 W 40-85 N	0.989	192.0	-3.0	62%
JGP95E	90-0 W 40-85 N	0.992	157.0	-7.0	54%
control data	90-0 W 40-85 N	0.998	84.5	-2.0	14%
Smith & Sandwell	90-0 W 40-72 N	0.996	118.5	-14.0	38%

Table 2.2: Comparison of bathymetric models for Greenland. The GGM-derived predictions from the FAGA of Andersen and Knudsen [1998] significantly surpassed all other bathymetric data sets when compared at the 257,941 bathymetric check points. Because the FAGA only extend to 80°N, the bathymetric predictions likewise only extend to 80°N. Bathymetry resulting from the gridding of the 257,939 control points produced good agreement with the check points but had an RMS difference that was 14% greater than the GGM predictions. The bathymetric predictions of Smith and Sandwell [1997] are also given below but are compared only for check points south of 72°N. Statistics of the comparison include the coefficient of correlation (CC), the RMS difference, and the mean difference. The percent (%) improvement of the GGM-derived bathymetry relative to the other bathymetric models is also given as defined by % improvement = $\frac{RMS_i - RMS_{GGM}}{RMS_i}$x 100.

Additionally, the bathymetric predictions from Smith and Sandwell [1997] are provided in Figure 2.22, although they're complete only up to 72°N. The performances of the various bathymetric models were compared next at the check points and are tabulated in Table 2.2.

According to Table 2.2, the GGM-predicted bathymetry represents an improvement over all the other models in terms of the RMS difference at the 257,941 check points. The GGM bathymetry show about 62% improvement over the EOTOPO5U data and a 54% improvement over the JGP95E data.

Table 2.2 also compares the grid generated by minimum curvature on the 257,939 control points. These estimates are well correlated with the check points but were more degraded in the RMS difference than the GGM bathymetry. These results suggest that the gridding algorithm has modeled the wavelengths well, but is not

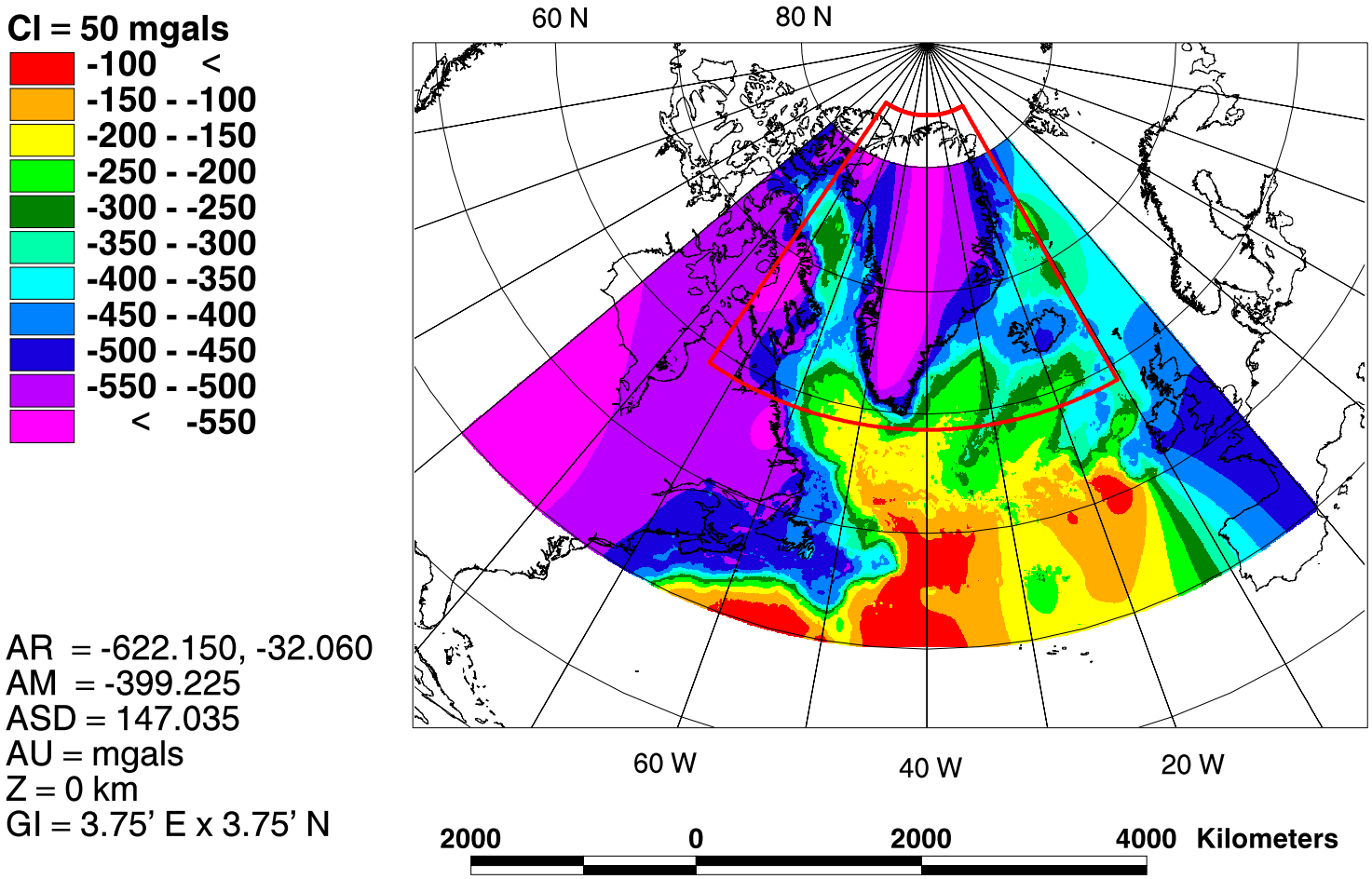

Figure 2.15: Regional bathymetric gravity effects (g_{REG}) for Greenland from combined NGDC and GSC bathymetric control data. The gravity effects are shown in a Lambert Equal-Area Azimuthal Projection centered on 40° W.

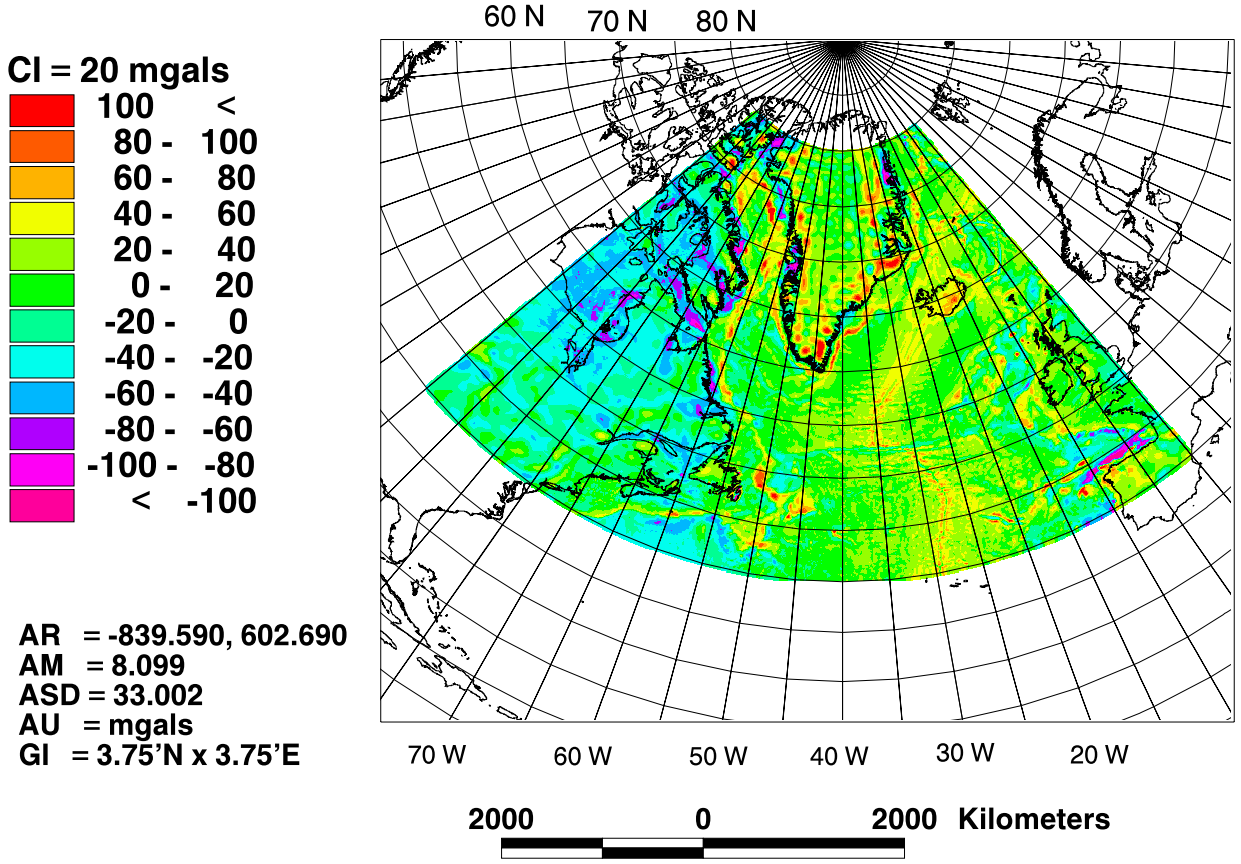

Figure 2.16: Standard FAGA from Andersen and Knudsen [1998] (g_{OBS}) for Greenland in a Lambert Equal-Area Azimuthal Projection centered on 40° W.

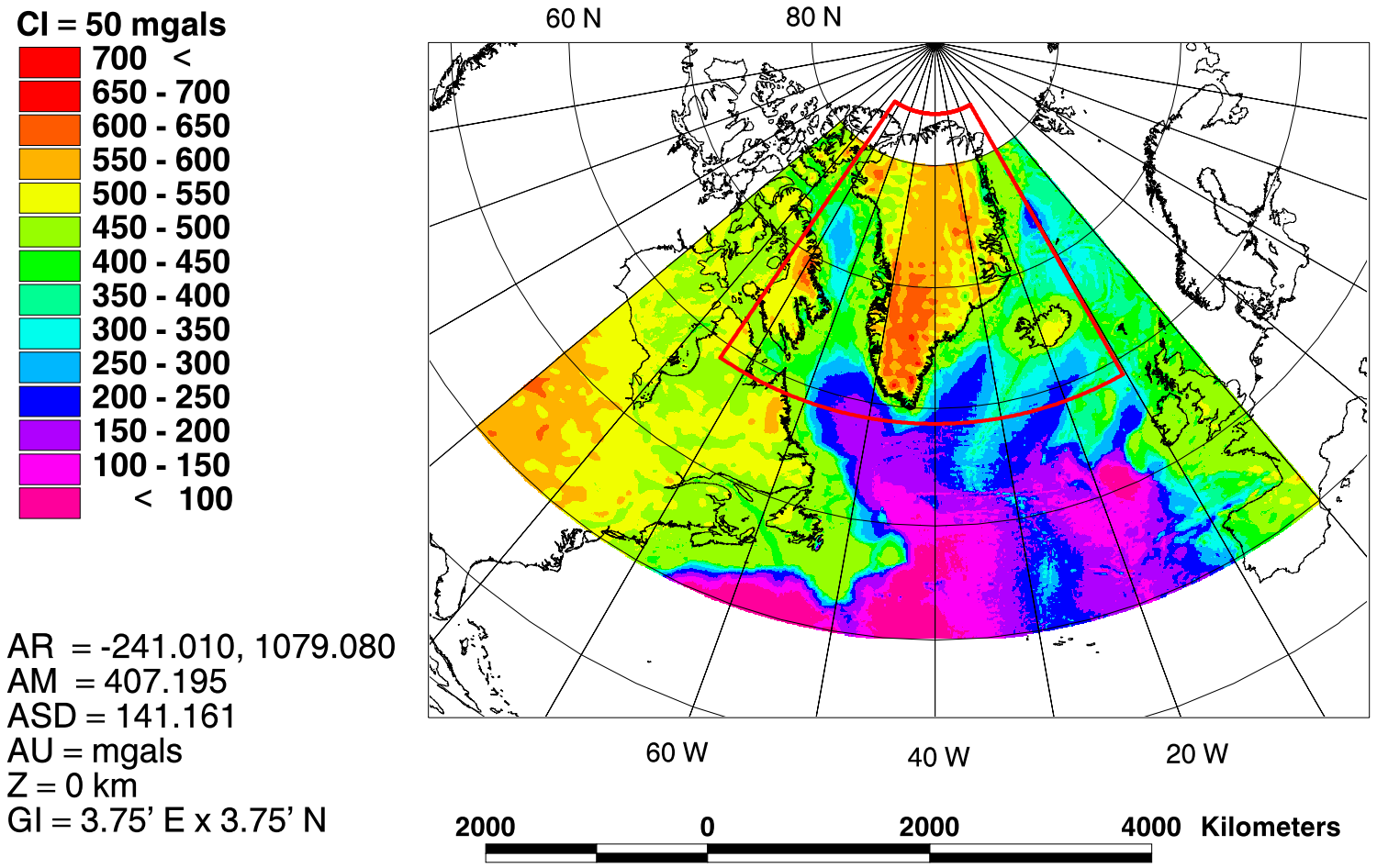

Figure 2.17: Residual bathymetric gravity effects (g_{RES}) for Greenland determined by removing the regional (g_{REG}) from the standard FAGA (g_{OBS}). The gravity effects are shown in a Lambert Equal-Area Azimuthal Projection centered on 40° W.

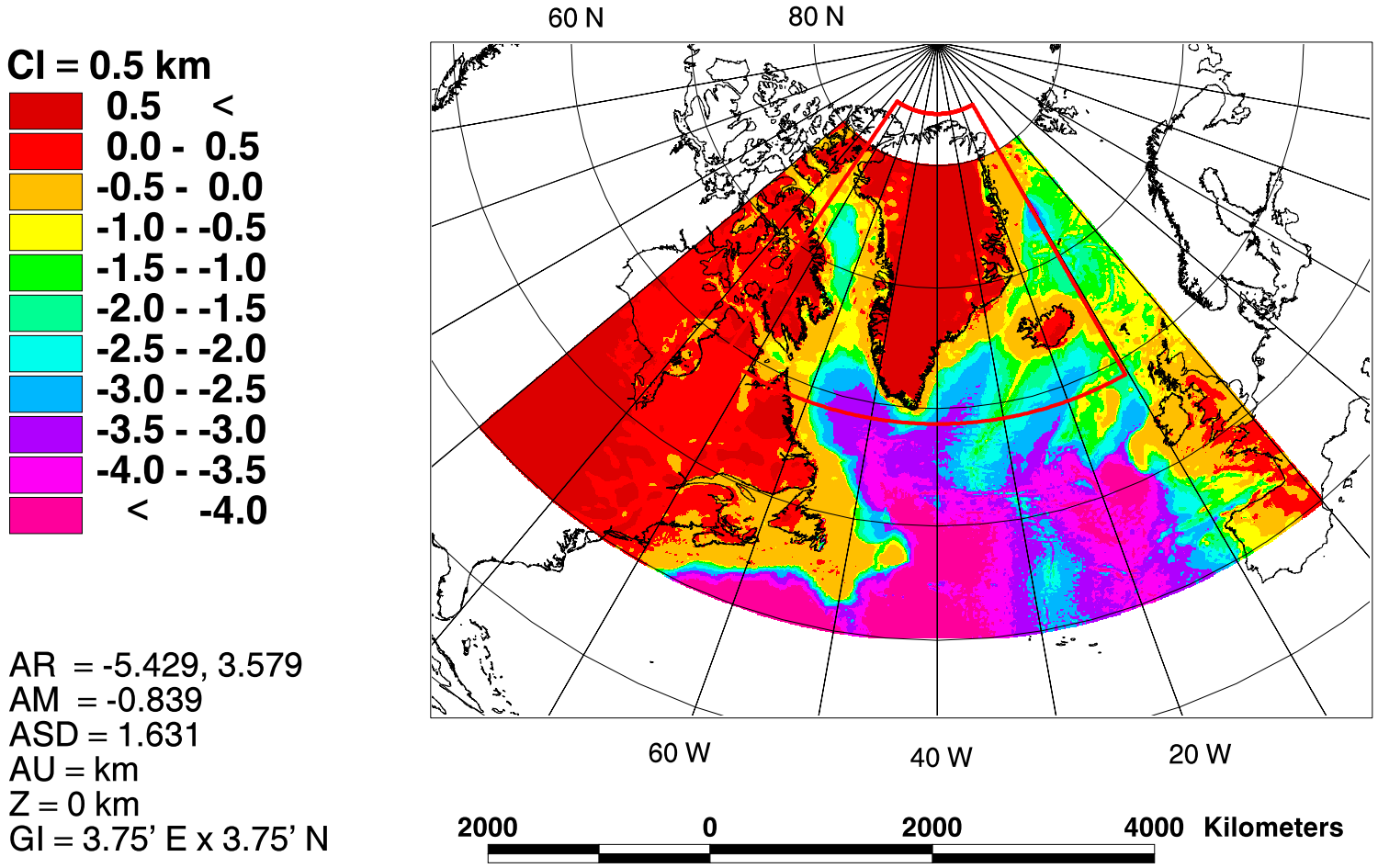

Figure 2.18: GGM-predicted bathymetry for Greenland in a Lambert Equal-Area Azimuthal Projection centered on 40° W.

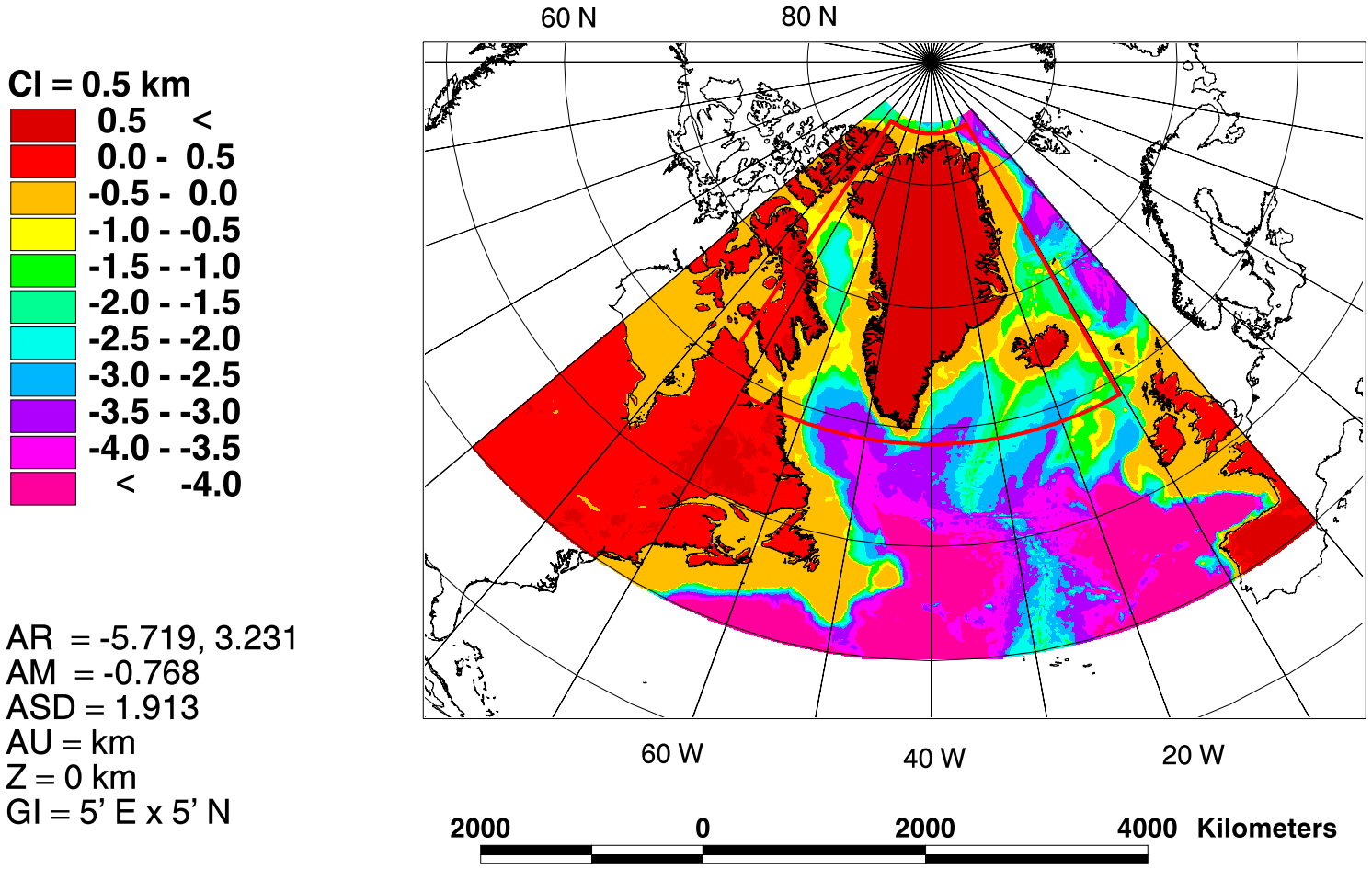

Figure 2.19: EOTOPO5U bathymetry for Greenland in a Lambert Equal-Area Azimuthal Projection centered on 40° W.

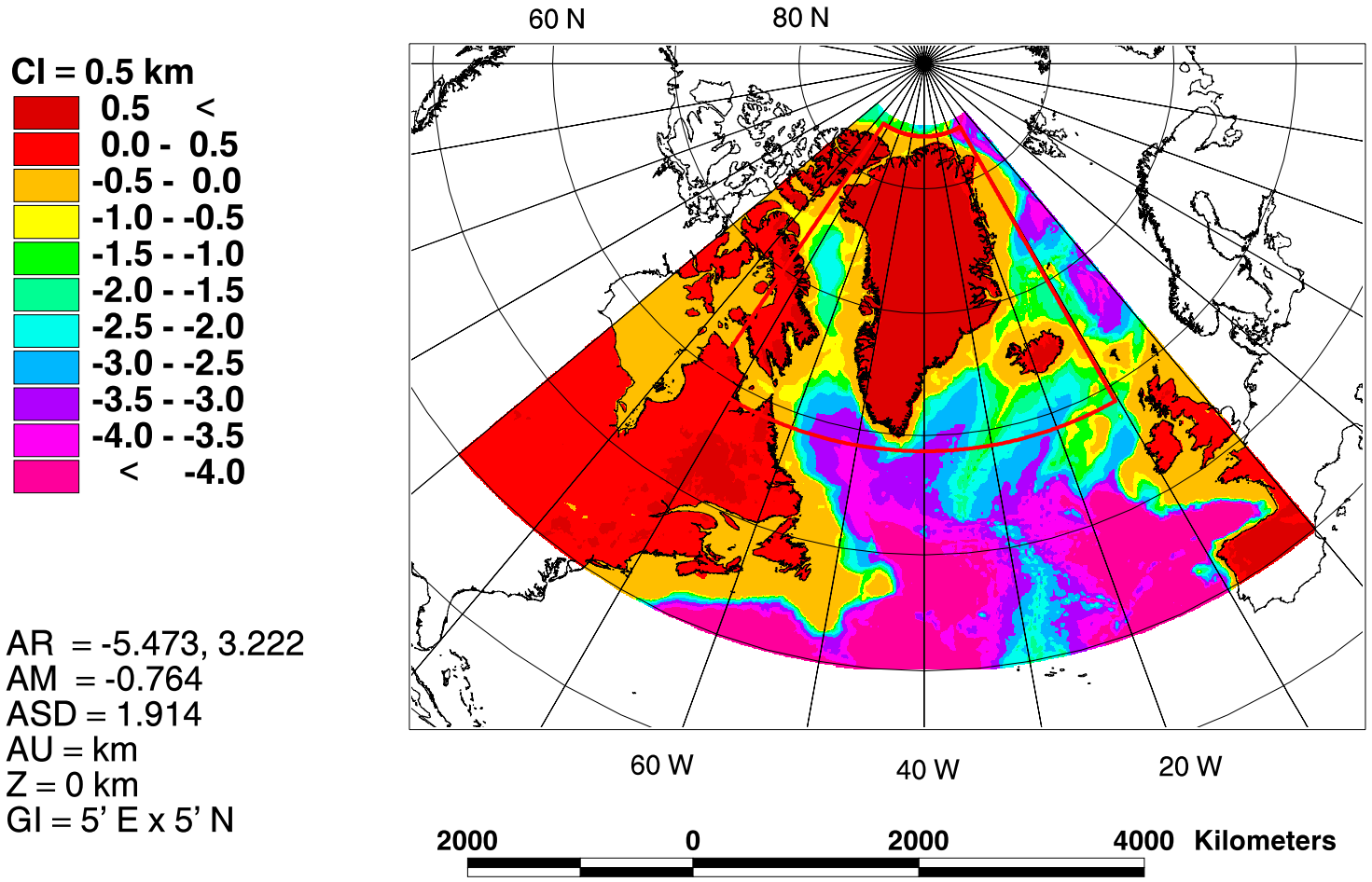

Figure 2.20: JGP95E bathymetry for Greenland in a Lambert Equal-Area Azimuthal Projection centered on 40° W.

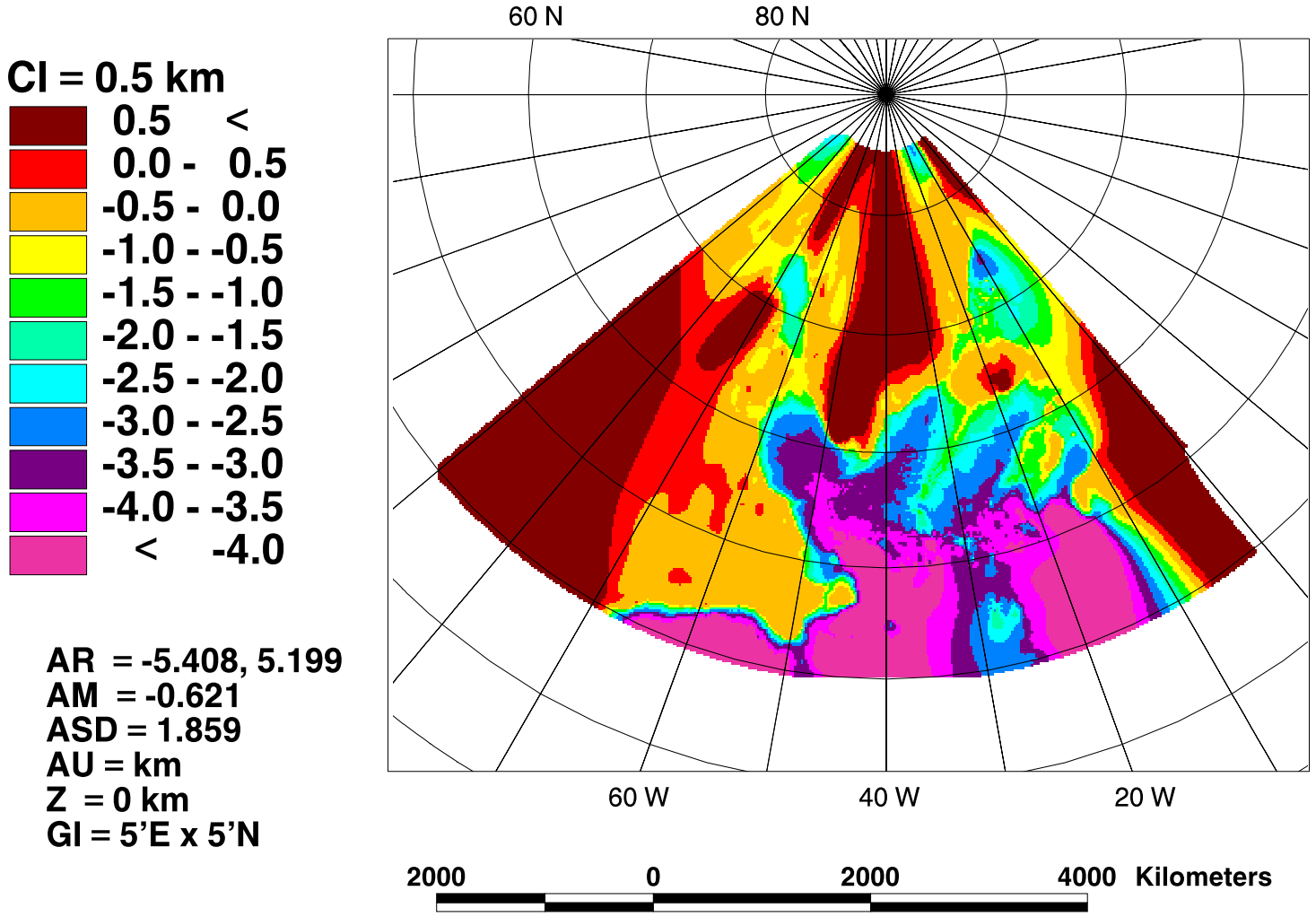

Figure 2.21: Greenland bathymetry from minimum curvature gridding of the 257,939 control points shown in a Lambert Equal-Area Azimuthal Projection centered on 40° W.

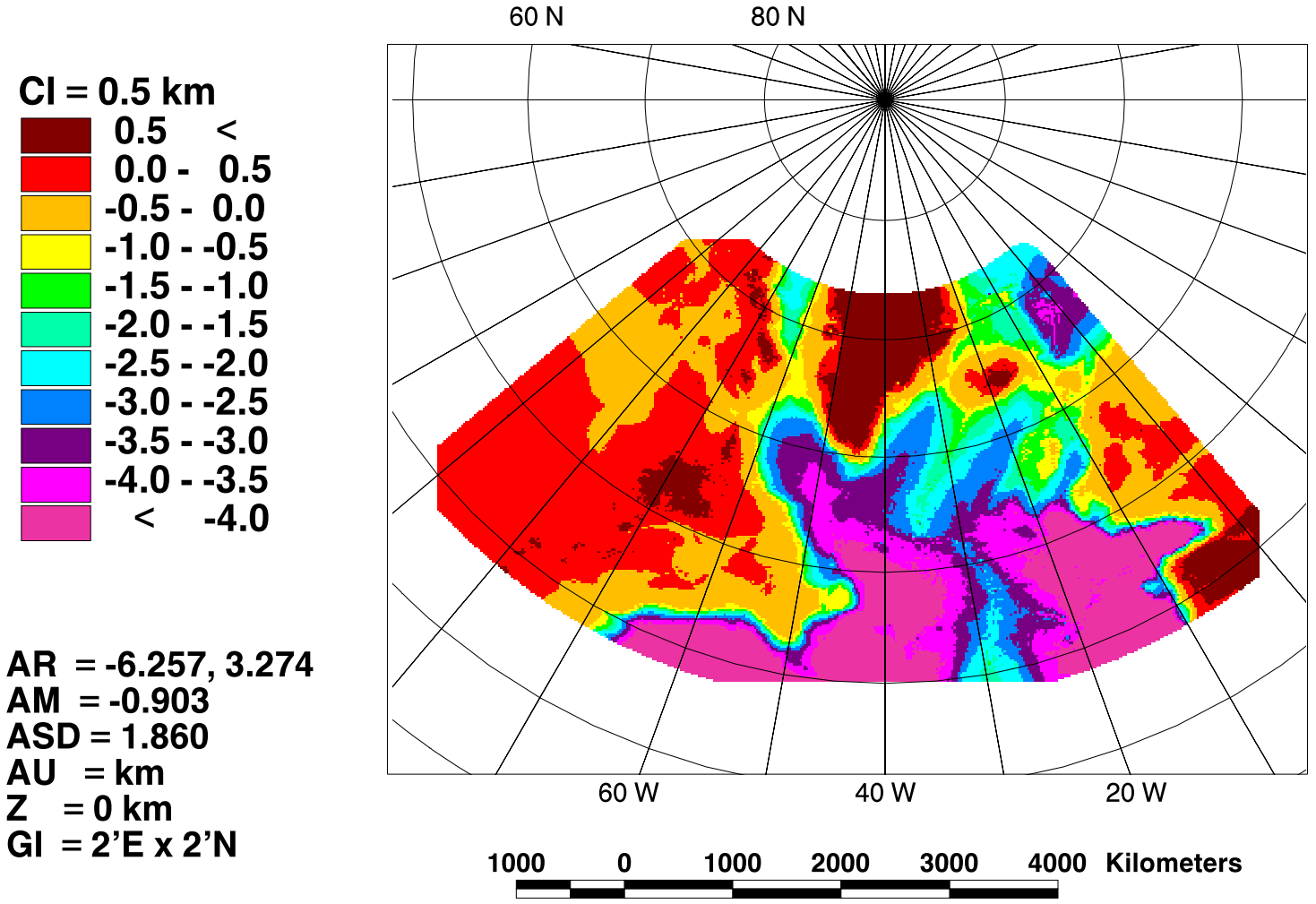

Figure 2.22: Greenland bathymetry from Smith and Sandwell [1998] in a Lambert Equal-Area Azimuthal Projection centered on 40° W.

matching the bathymetric amplitudes well. The FAGA apparently constrain the bathymetric amplitudes better, particularly as the relief increases [Nagarajan, 1994]. Additionally, the incomplete coverage provided by the bathymetric control points shown in Figure 2.14 will probably result in inferior predictions in the gaps, as noted in the southeastern margins of Figure 2.21.

2.5 Conclusions

The Gravity Geologic Method (GGM), which has been applied previously to estimating bedrock depths beneath unconsolidated materials, can be readily adapted for mapping sea floor topography. This approach yields effective bathymetric predictions by combining known bathymetry available from ship soundings or other observations with marine free-air gravity anomalies (FAGA) determined from shipborne or satellite altimetry surveys.

The role of the GGM for bathymetry mapping was investigated in both shallow and deep sea environments. In shallow marine environments like the Barents Sea, bathymetric gravity effects are likely in the higher frequency perturbations of the gravity field relative to the more subdued effects of deep water bathymetry.

Hence, to develop the Barents Sea predictions, ERS-1 altimetry were re-processed for the higher frequency components that were added to the standard FAGA of Andersen and Knudsen [1998]. However, the bathymetric predictions determined using the GGM from these enhanced FAGA were nearly identical to those generated using only the standard FAGA. Differences between these GGM-derived bathymetric predictions were generally less than one meter, which was significantly smaller than the 25.5 m RMS difference determined for both of these predictions with the check data.

The GGM-derived predictions were both better than the bathymetric predictions from the EOTOPO5U and JGP95E models, which had RMS differences of 35.3 m

and 34.9 m, respectively. The bathymetric predictions estimated by simply gridding the 218 control depths had a 30.8 m RMS difference, which was also greater than that of either of the GGM-derived bathymetric predictions.

These results suggest that the GGM can be used to generate improved bathymetric predictions for shallow marine environments. They also suggest that the standard FAGA may be sufficient for making these predictions without further enhancing the higher frequency components of the FAGA signal.

The GGM was also tested for mapping deep water bathymetry around Greenland, where predictions from various other models were also available for comparison. Only the standard FAGA of Andersen and Knudsen [1998] were used to make the GGM-derived predictions in this region due to the similarity of the results in the Barents Sea region.

Again, the GGM-derived bathymetry surpassed that of all other comparison bathymetric data sets. The 73.7 m RMS difference between the GGM bathymetry and the 257,941 check points was improved over both the EOTOPO5U and JGP95E models, which had RMS differences of 192.0 m and 157.0 m, respectively. The bathymetric predictions of Smith and Sandwell [1997] cover the middle and southern portion of this field area and had a 118.5 m RMS difference with the check points. Finally, the bathymetry determined by gridding the 257,939 control points had a 84.5 m RMS difference but seemed to contain poorer quality regions related to the gaps in the coverage.

For the shallow marine environment of the Barents Sea, a geologically unreasonable density contrast of 20.0 gm/cm^3 was found to generate the best bathymetric predictions. For the deeper waters around Greenland, the more reasonable value of 2.06 gm/cm^3 was sufficient. This necessity for an extreme density contrast value in the shallow environment may be related to the narrow range of depths and the

need to enhance the contrast at the boundary. For deeper waters, where a greater bathymetric range occurs, no geologically unreasonable estimate was necessary.

In general, the Gravity-Geologic Method appears to a sufficient tool for making bathymetric predictions in both shallow and deep marine environments. The ready availability of global marine FAGA data sets provided by Andersen and Knudsen [1998], Sandwell and Smith [1997], and others ensures that the GGM can be used in conjunction with ship track bathymetry to extend the coverage into unmapped regions, which should generate better results than simply gridding the data or relying upon global data sets.